

Analyzing the Effect of Temperature on Alloy Steel Forging Simulation Using Finite Element Simulation

DAME Alemayehu Efa^{1,a}, HIRPA G. Lemu^{2,b*},
ENDALKACHEW Mosisa Gutema^{1,c} and MAHESH Gopal^{1,d}

¹Department of Mechanical Engineering, College of Engineering and Technology, Wollega University, Nekemte P.O. Box 395, Ethiopia

²Department of Mechanical and Structural Engineering and Materials Science, Faculty of Science and Technology, University of Stavanger, N-4036 Stavanger, Norway

^adameeifaa@gmail.com, ^bhirpa.g.lemu@uis.no, ^cendalkem5@gmail.com,
^ddoctorgmahesh@gmail.com

*Correspondence: hirpa.g.lemu@uis.no

Keywords: AISI 4120 alloy steel, Metal forming simulation, Open die forging process, Deform-3D, Inter-object, Plastic deformation.

Abstract. The goal of this research is to examine the influence of temperature affects the forging of a rectangular billet of AISI 4120 alloy steel using the 3D Deform version 11 software. The simulation was performed with 0.3 coefficient of friction on a metal forming (lubricated) process and the part is intended for application in aerospace and oil and gas industries. Three modules of deform software were defined to execute the simulation: pre-processing, simulation, and post-processing. The pre-processing in forging employed standard data— material selection, billet drawing, top and bottom dies design, meshing and simulation control. After 120 steps, the post-process estimation of deformation temperature, effective strain and stress, total velocity, and total displacement were obtained on the billet of material at temperatures of 800° C, 1000° C, and 1200° C. The results show that when forging temperatures climb, effective strain and stress decrease, total displacement and velocity decrease, and the final temperature increases.

Introduction

Metal forming refers to manufacturing process that transforms a given material, generally shapeless or of simple geometry, into a valuable item without changing the material's mass and composition. The obtained geometric part is often complicated in geometry, with well-defined shape, size, accuracy and tolerances, appearance, and qualities. Metal forming procedures such as rolling, forging, extrusion, and drawing involve significant plastic deformation posing difficulties for analytical analysis. DEFORM-3D software is an innovative process for studying the three-dimensional (3D) flow of difficult metal forming processes. It is a vital and practical tool for forecasting flow of material in industrial forming processes without high cost and time delay of shop trials. DEFORM, which is based on FEA, has been shown to be accurate and robust in industrial applications over several decades. The simulation can accurately forecast large deformation material flow and thermal behaviour. In previous studies in [1], [2], DEFORM-3D simulation software was used to anticipate forming faults in the mold steel of 65Ne gear in a cold closed-die forging process. DEFORM 2D/3D-FEM method was used and conducted comparison of analytical and numerical methodologies for a forging process, including friction, reduction ratio, and the effect of billet shape [3]. The author in [4] performed a finite element method (FEM) based simulation in die forging of a NIMONIC 80A material using DEFORM 3D to decrease the temperature on the sheet edges and transverse fractures on the surface. 3D FE-based numerical approach sensitivity analysis was utilized to explore the forging process of Ti-6Al-4V ingot to assess the influence of press speed, feed, and reduction on workpiece deformation and effective strain [5]. DEFORM software was used to simulate temperature, press travel velocity, and friction factor to study the processes of die forging of AK6 aluminum alloys [6]. Using Deform 3D simulation software, [7] lowered the stress intensity and deformation intensity of the forging die to increase cavity fill and minimize waste in metal burrs of steel 40 GOST 1050-88.

DEFORM-3D software was also utilized to analyze the experimental and finite element simulations of a forging operation's compression finishing and ironing finishing, and the helix angle affected the difference in tooth form and surface quality of both tooth surfaces of each gear [8]. The authors in [9] assessed the possibilities of reducing working forces, minimizing load, and increasing tool life or press capacity in precision metal forming procedures. The authors in [10] used the FEA approach in the forging modeling process using Deform Software of an aluminum alloy swing arm to save cost. The die stress analysis was performed using the DEFORM 3D by differing the temperature of the die while maintaining the heat of the workpiece as a constant, forming a procedure to investigate the effect of variables on the performance features and the influence of initial die temperature on die stress [11]. The authors in [12] optimized the forging numerical simulations of X20 steel utilizing the Deform 3D software and the optimization was carried out using the Taguchi method and ANOVA method to examine the deformation of the cylinder.

By comparing simulation results with actual components, the author in [13] investigated the numerical simulation of the forging process in Deform 3D. The fact that the dies and workpiece geometry were properly constructed and filled the workpiece cavity space of the dies means that the simulation results mostly match the actual ones. The authors in [14] used DEFORM software to simulate the 21 - 4N valve dies forging process and investigated the simulation results of optimal process parameters such as temperature, speed, and frictional force coefficient. The authors in [15] studied using Deform 3D to execute forging process performance of 40 GOST 1050-88 steel convex dies. The authors in [16] used DEFORM 3D simulation of Nimonic 115 to assess fatigue strength and creep resistance. As a result, the first heat transfer process significantly impacted the material's deformation behavior. The authors in [17] compared the results to the tensile strength obtained using JMatPro[®] software and the maximum principal stress derived with DEFORM-3D software.

DEFORM 3D is also widely used to analyze temperature, stress, strain, velocity and displacement during simulations. For instance, plastic deformation properties of 42CrMo steel was used as a material in upsetting process to determine the possibility of employing DEFORM-3D software computer simulation to examine temperature, stress, and strain changes, as well as forming flaws [18]. The authors in [19] investigated temperature, stress, strain, velocity, and metal flow condition in a forging process for a vehicle front axle, whereas [20] investigated process parameters such as temperature using thermomechanical techniques in conjunction with strain rate and microstructure evolution. The microstructure evolution is done using optical microscopy in a warm forging of a low carbon steel using DEFORM-3D software. The authors in [21] experimented the plastic deformation behavior of 1.4922 stainless steel of a forging using Deform 3D software to investigate the effect of forging temperature. The data highlighted that higher forging temperatures result in lower deformation resistance and that maximum effective stress and strain decreases as forging temperature increases. The authors in [22] used Deform-3D simulation software to study the temperature, strain, and stress distribution of X20CrMoV121 steel during a forging process. As a result, deformation inhomogeneity reduced as the strain rate increased. The strain, stress, total velocity, displacement, and temperature of 17Cr-13Ni-2Mo and 17Cr-5Ni-5Mo-Ti alloyed steel billets [23] and Ti-6Al-4V billet [24] were determined using Deform-3D software and a comparison of performance characteristics at various billet temperatures was performed. The authors in [25] used DEFORM 3D FEM software to simulate the temperature field, strain, and shear strain during TIMETAL 685 forging. This experiment demonstrated that the needed creep qualities should meet using the non-isothermal processing technique with the correct thermomechanical process parameters selection. The experiment was conducted on AISI1045 steel end-milling with a tungsten carbide tool and used finite element analysis-based modeling using DEFORM-3D software to minimize temperature, stress, thrust force, tool wear geometry, and strain [26].

The review of recent literature shows that there exists limited publications on simulation experiments using AISI4120 alloy steel material in open-die forging at forging temperatures of 800° C, 1000° C and 1200° C. Thus, this research is intended to contribute to the research gap and be helpful to industrialists and researchers. The pre-processing and post-processing simulation was

done to predict effective strain and stress, velocity, total deformation, and final temperatures using DEFORM 3D software.

1.1 Mathematical model

In the metal forging process, a mathematical model is used to simulate and optimise process variables throughout production, analyse the behaviour of the material, and anticipate the effects of forging conditions. The activation energy, which is given in equation 1 represents the plastic deformability of the material and it is critical for understanding energy and temperature issues in the metal forging process [27].

$$E_a = 2.303R \left\{ \frac{\partial \log \sigma}{\partial \left(\frac{1}{T} \right)} \right\}_{\dot{\epsilon}} \left\{ \frac{\partial \log \dot{\epsilon}}{\partial \log \sigma} \right\}_T \quad (1)$$

Where $\frac{\partial \log \sigma}{\partial \left(\frac{1}{T} \right)}$ refers to the gradient of $\log \sigma$ and $1/T$ at various strain rate ($\dot{\epsilon}$) and $\frac{\partial \log \dot{\epsilon}}{\partial \log \sigma}$ refers to the gradient of $\log \dot{\epsilon}$ and $\log \sigma$ at various deformation temperature.

The forming process uses the Johnson-Cook material model and the Lagrangian incremental (LE) method of mathematical formulation. Equation 2 illustrates the strain rate and temperature dependent equation for the work piece's isotropic behavior with deformable thermo-viscoplastic property [26].

$$\sigma_f = \left[1 - \left(\frac{T - T_{ref}}{T_m - T_{ref}} \right)^m \right] (\sigma_{yi} + B \epsilon^n) \left(1 + C \ln \frac{\dot{\epsilon}}{\dot{\epsilon}_0} \right) \quad (2)$$

Where T, T_{ref} and T_m , are equivalent, reference and melting temperature ($^{\circ}\text{C}$), σ_f and σ_{yi} are flow and initial yield stress (MPa), B is hardening modulus and ϵ, n, C and ϵ are plastic, hardening exponent and coefficient of strain rate.

The viscoplastic equation, which is represented by equation 3, describes the properties of the material under various plastic and elastic loading conditions during the forming process [21].

$$\delta \varphi = \int_v \sigma_e \delta \dot{\epsilon}_e d_v + \int_v K \dot{\epsilon}_v \delta \dot{\epsilon}_v d_v - \int_{sf} F_i \delta u_i d_s = 0 \quad (3)$$

Where σ_e and $\dot{\epsilon}_e$ are the effective stress and strain, $u_i, sf, F_i, \dot{\epsilon}_v$ and K are surface velocity (m/s), surface force (N), traction stress (MPa), volumetric strain and penalty factor.

The Fourier energy balance, as shown in equation 4, can be used to estimate the temperature distribution of the deformation process.

$$\rho C_p \frac{\delta T}{\delta t} = \nabla^T (K \nabla T) + \dot{Q} \quad (4)$$

Where K, T, \dot{Q}, ρ and C_p are conductivity ($\text{W}/\text{m}^{\circ}\text{C}$), temperature ($^{\circ}\text{C}$), heat generated (J), density of material (kg/m^3) and specific capacity of heat ($\text{J}/\text{kg}^{\circ}\text{C}$).

2. Materials and Methods

2.1 Material data and preprocessing

For the simulation a rectangular AISI4120 alloy steel with dimensions length, width, and height of 50 mm \times 50 mm \times 130 mm and two dies with dimensions length, width, and height of 90 mm \times 90 mm \times 25 mm and 10 mm corner radius were used. The DEFORM-3D software basic modeler was used to generate material inter-object material data, which was then used to determine the link between the changes from one phase to the next. Using the DEFORM 2D User's Manual, [28] proposed material data, Pre-Processor, and Post-Processor simulation techniques. The DEFORM material library was used to choose the temperature range for AISI 4120 alloy steel [70-220 F (20-1200 $^{\circ}$ C)], while the JMatPro - Sente Software was used to test the AISI4120 alloy steel properties, as shown in Fig. 1.

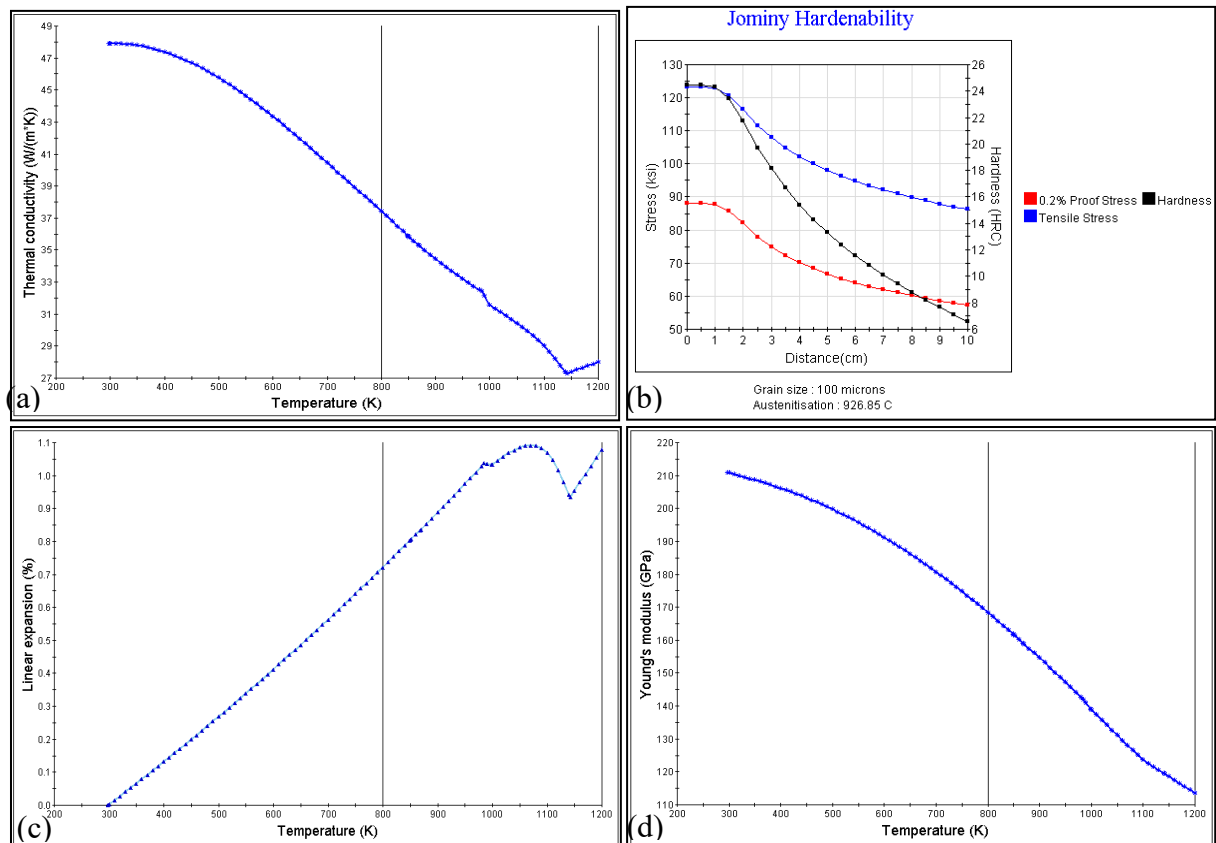


Fig. 1. AISI4120 alloy thermal and physical properties

The structural analysis was performed using a finite element model consisting of 8234 points, 6444 polygons, and 6674 nodes generating volume with 29320 elements, considering three noded triangular elements.

Fig. 2 (a, b) shows a meshing model for the open-die forging with a billet between two dies. The bottom die is rigid; a hydraulic press moves the top die at a forging speed of 5 mm/s. The following controls were used to run the simulation:

- number of steps = 120,
- step increment = 10, and
- Control time = 0.01 sec/step increment.

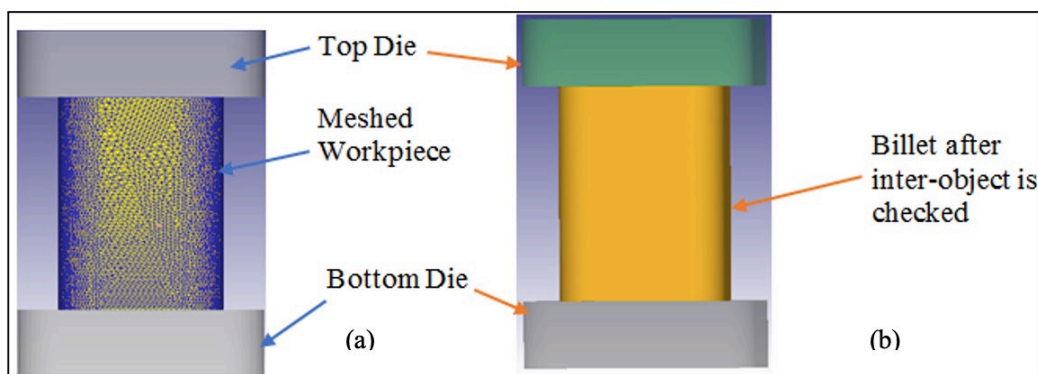


Fig. 2 a) Open die forging model with meshed billet; b) Billet position between top and bottom dies

Shear type friction was often considered due to the material's tendency to shear during bulk deformation operations, and typical friction values range between 0.2 and 0.9. Thus, a friction coefficient of 0.3 was chosen to mimic the common usage of graphite lubricant between the die and material [21]. The inter-object forging assembly of components specification is shown in Fig. 3 (a). A "database" is the primary data storage location for both original input and selected solution steps, and it encompasses the whole simulation set of data, including simulation control, object data,

relational inter-object data, and material data [28]. The database was successfully generated, as shown in Fig. 3 (b). This investigation used an increment-type Lagrangian isothermal simulation technique at 20° C (local ambient temperature is 25° C), 200° C die temperature, and a heat transfer coefficient of 8 W/m²/K.

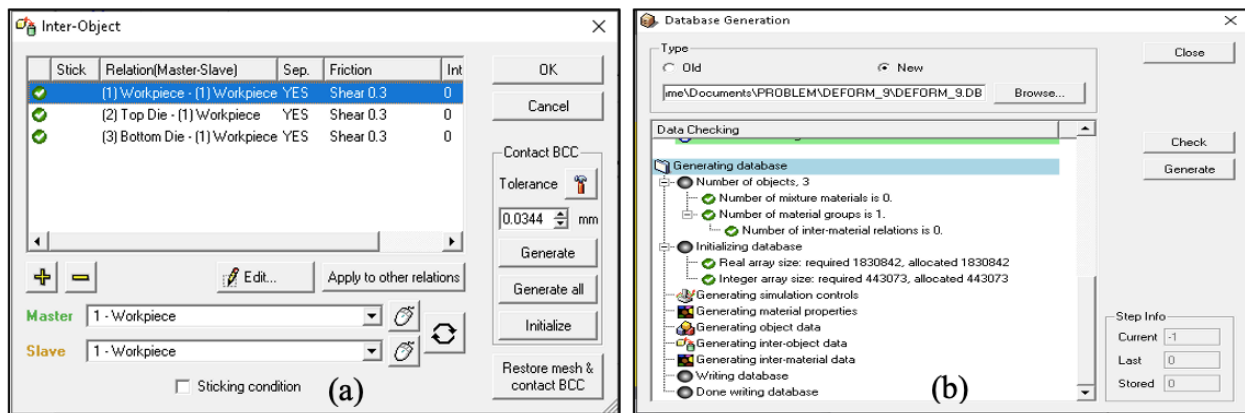


Fig. 3. a) Forging assembly of parts definition of the inter-object b) Database generation

2.2. Simulation and post-processing

The simulation engine computes numerically; 120 simulation steps (illustrated in Fig. 4) were executed by receiving input data from the database and displaying the simulation result. During the simulation, message and log files were created. The log file handles general information, re-meshing, and error messages at the beginning and finish.

The simulation data was then displayed via a graphical user interface in the post-processing phases to view the results of total displacement, total velocity, effective stress, strain, and forging temperature. The simulation was performed with different temperatures to obtain varied forging temperature results. Fig. 4 shows a typical simulation of the billet in various load stages to improve understanding of the billet's behavior before and after forging. The same method was used at temperatures of 800° C, 1000° C, and 1200° C.

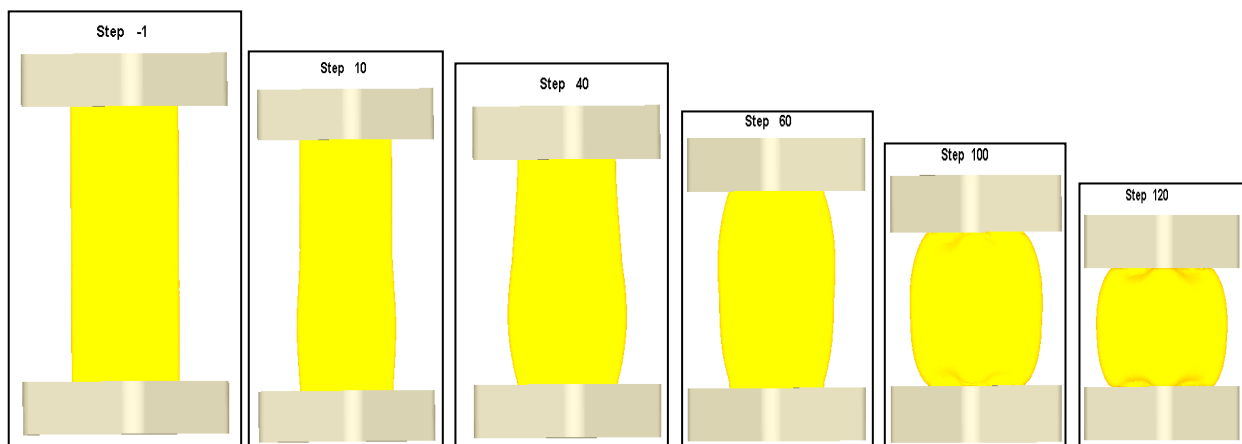


Fig. 4 Billet simulation before and after the application of various load steps

3. Results and Discussion

3.1 Results of the forging simulations

During the simulation the forging diameter was reduced from 130 mm to 25 mm. The stress, strain, total displacement, total velocity, and final temperature simulation results for the three selected temperatures are presented below together with their properties.

The results for the effective stress, total velocity, effective strain, total displacement, and final forging temperature at 800° C, 1000° C, and 1200° C are depicted in Fig. 5 Fig. 6 and Fig. 7

respectively. Summary of the results of the effective stress, total velocity, effective strain, displacement distributions and the final temperature after forging are also given in Table 1.

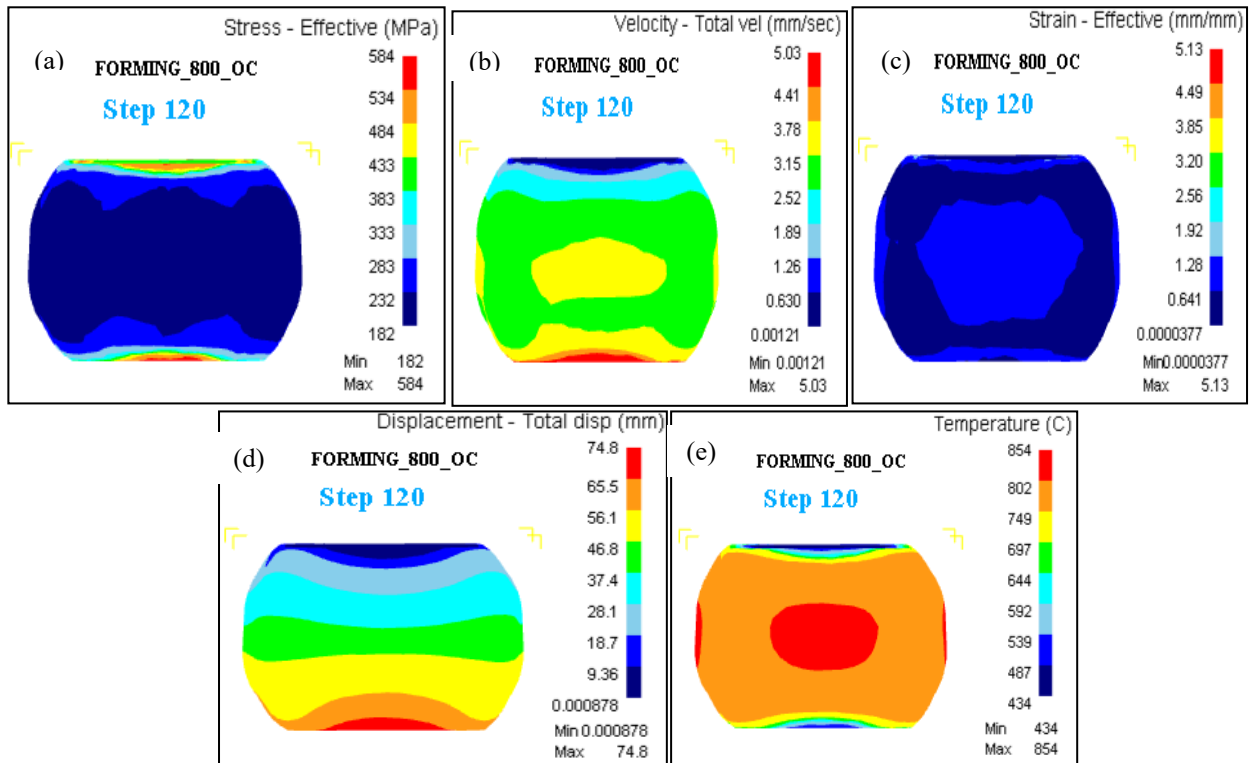


Fig. 5 Distribution of a) Effective stress, b) Total velocity, c) Effective strain, d) Displacement, and e) The final temperature after forging – at 800° C

Table 1 Summary of simulation results

Test temp. °C.	Effective stress, MPa	Total velocity, mm/s	Effective strain, mm/mm	Displacement, mm	Final temp.°C
800	584	5.03	5.13	74.8	854
1000	496	5.04	4.15	74.7	1010
1200	361	5.0	2.6	75	1190

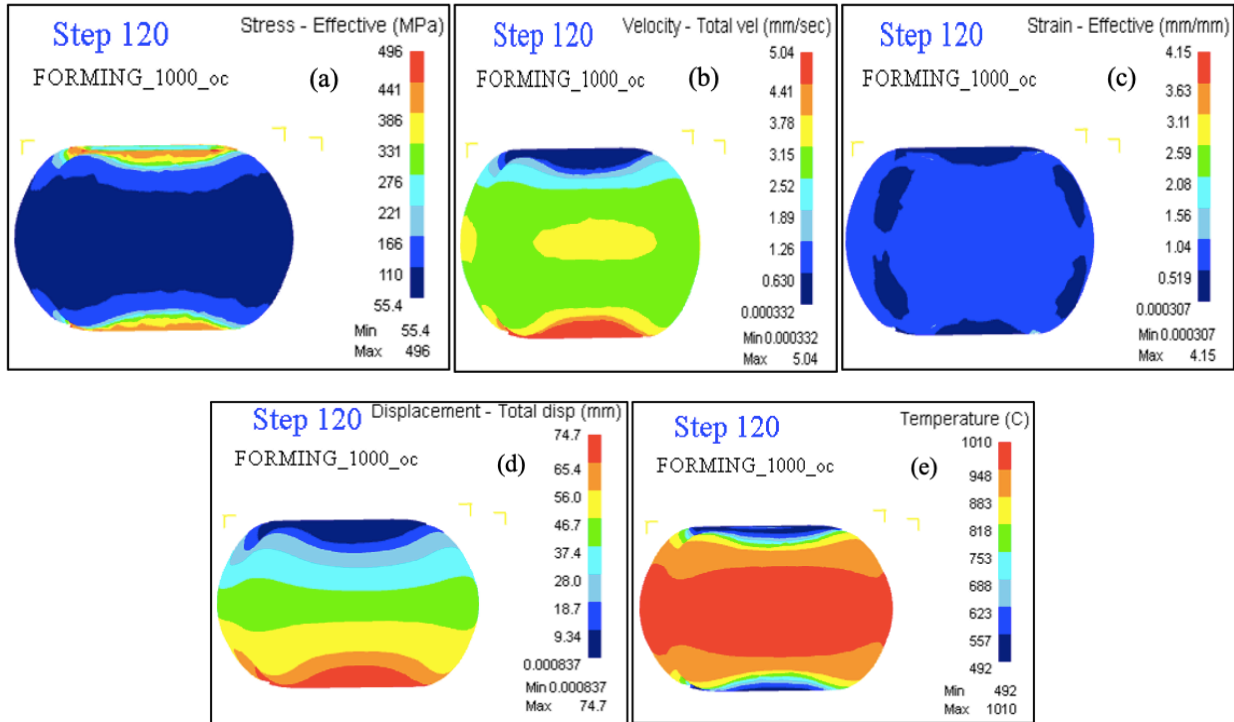


Fig. 6 Distribution of a) Effective stress, b) Total velocity, c) Effective strain, d) Displacement, and e) The final temperature after forging – at 1000° C

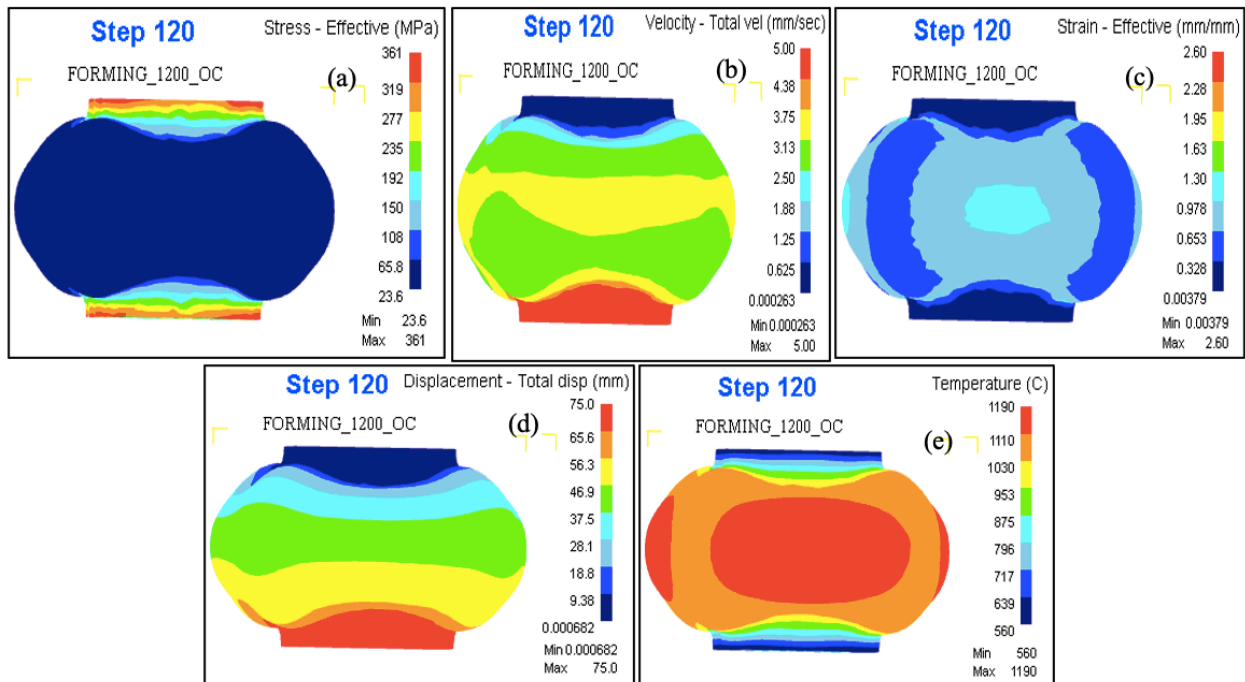


Fig. 7 Distribution of a) Effective stress, b) Total velocity, c) Effective strain, d) Displacement, and e) The final temperature after forging – at 1200° C

3.2. Discussion of results

During the finite element simulation, the entire forging operation took 14.94 seconds. Deformation was not spread uniformly over the three simulations (Figs. 5, 6, and 7), resulting in the formation of distinct zones such as the dead zone (less distorted), mild zone (moderately deformed), and shear zone (more deformed). From the results, when the forging temperature increased, the effective stress reduced from 584 to 496 MPa and then to 361 MPa at 800°C, 1000°C, and

1200° C, suggesting that the material deformed plastically. The flow of stress is high at the surface due to the minimum heat transfer but as forging temperature increased it reduced ([16], [18]).

As a result, effective strain decreased from 5.04 (mm/mm) to 5.00 (mm/mm), and stress and strain were directly proportionate, resulting in less plastic deformation and limited grain structure refinement. Finally, displacement and velocity decreased in all three trials, suggesting that the billet is resistant to deformation; load and forging temperature increased from step 1 to 120, and it becomes undeformable when an unreasonable load is obtained. The energy required for forging was decreased as the motion of the dislocation increased and the materials became softer as the temperature increased; at the same time, the size of the dislocation extended, hardening the work as experimentally shown by [29], [27].

As a result, forging stress increases, and temperature influences work hardening caused by increased dislocation [21],[23]. In this study, a plot of load (in N) vs stroke (in mm) was used to anticipate the actual forging load. The forging load reduced from 1 330 kN to 627 kN and then to 271 kN as the temperature climbed from 800° C to 1000° C and subsequently to 1200° C, as indicated in Fig. 8 (a), (b), and (c), and the similar proposal is offered by [2] , [24]).The coefficient of friction increased and approached one as the forging load gradually raised from lower stages to higher steps up to 60 mm stroke. As the coefficient of friction increased, the temperature increased, softening the workpiece.

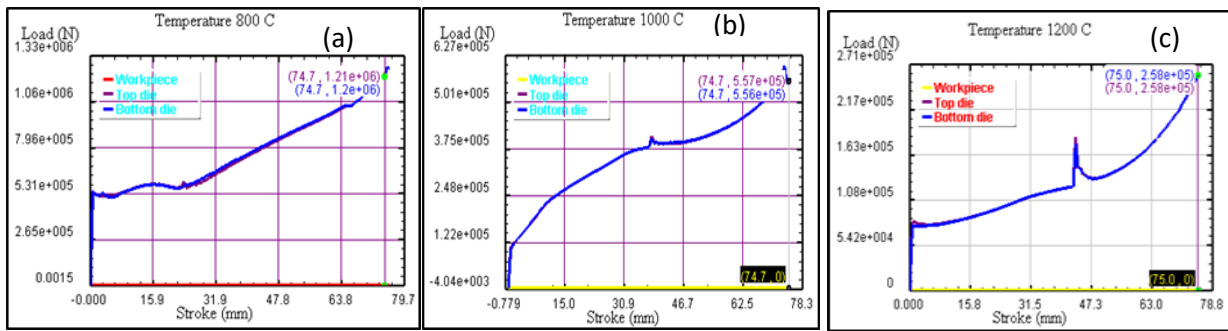


Fig. 8 Forging load versus stroke curves a) 800° C, b) 1000° C, c) 1200° C

In hot forging, it is expected that the load progressively increases and the flow stress eventually increases [30], while the coefficient of friction at the interface of dies and work pieces varies[31]. The results depicted in Figs 5, 6, and 7 indicate that the effective stress and strain flow did not remain constant from step to step when AISI 4120 alloy steel was forged at temperatures of 800° C, 1000° C and 1200° C. The final value of the effective stress is higher at the lowest effective strain value, and vice versa, similar to what was reported by [27], [24]).

As illustrated in Fig. 9 and Fig. 10 the effective stress develops rapidly at temperatures of 800° C, 1000° C, and 1200° C; the ultimate stress value is attained, and the strain value becomes minimum. Furthermore, after the completion of the final value, the stress value decreases, but the effective strain value progressively increases, and vice versa [18], [24].

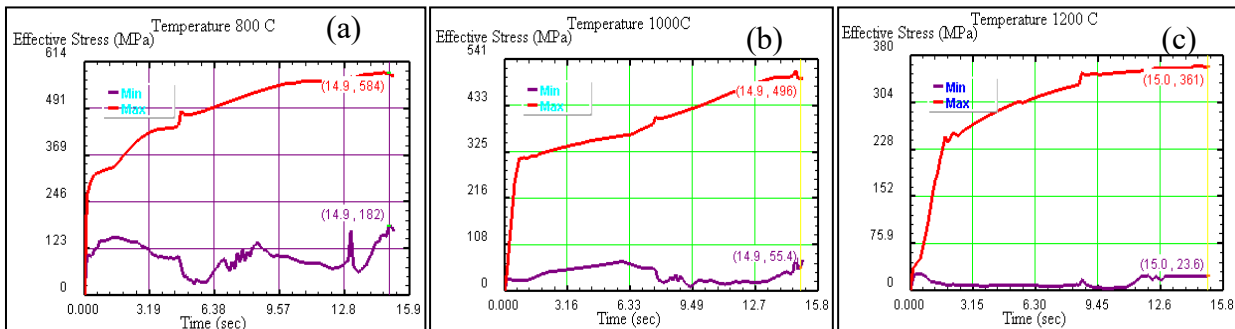


Fig. 9 Effective stress-curves

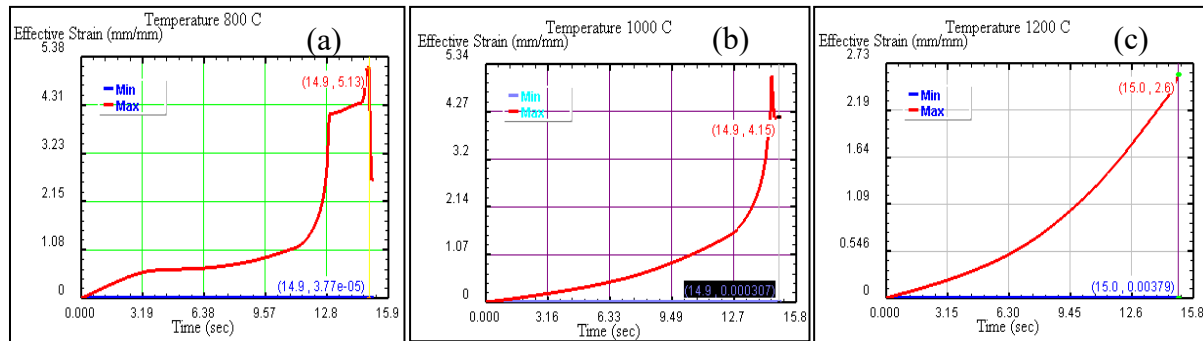


Fig. 10 Effective strain- curves

Based on the study's findings, when forging temperature rises, a minimum forging load is applied, and as forging temperature rises, effective stress decreases. Increasing the temperatures of the billet forging decreases effective stress, lowering the temperature at which deformation occurs. The effective strain causes the least amount of plastic deformation and restricts the refinement of grain structure. Total velocity and displacement have excellent deformation resistance[24].

During pre-processing of this experiment, however, a velocity of 5 mm/s was used and the findings indicated that the velocity at the edge differed from the velocity at the intermediate or lowest region. The position of the particle within the deforming material affects the particle's overall velocity. The particles at the edge of the workpiece were found to move at a higher velocity than the particles in the middle region, while the particles towards the bottom of the billet moved at a lowest overall velocity [21], [23]. As a consequence, at temperatures of 800° C, 1000° C, and 1200° C, the velocity at the edge exceeds the velocity at the intermediate, and the intermediate velocity exceeds the velocity in the lowest zone Fig. 11.

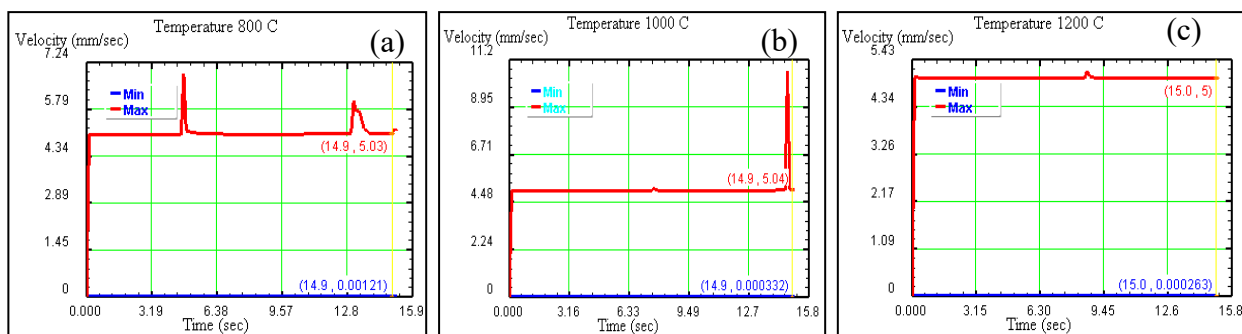


Fig. 11 Plots showing the billet's total velocity at a) 800° C, b) 1000° C, c) 1200° C

Figures 12 and 13 illustrate the standard deviations of the effective strain and stress distributions, indicating that the deformation process did not result in inhomogeneous deformation. Internal heat is generated as a result of friction effects at the die-workpiece contact, resulting in inhomogeneous deformation[24]. Deformation inhomogeneity and effective strain formed as a result. Since the internal temperature is higher than the exterior temperature, the heat generated is lost through the specimen's surface. Similar to the observation reported by [22], the degree of deformation and flow inhomogeneity are directly related, implying that as flow inhomogeneity increases, consequently the degree of deformation.

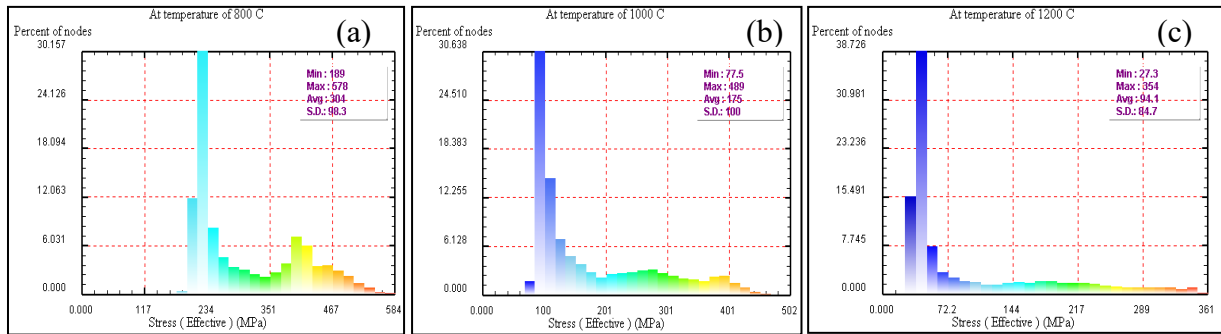


Fig. 12 Effect of die movement on the effective stress distribution

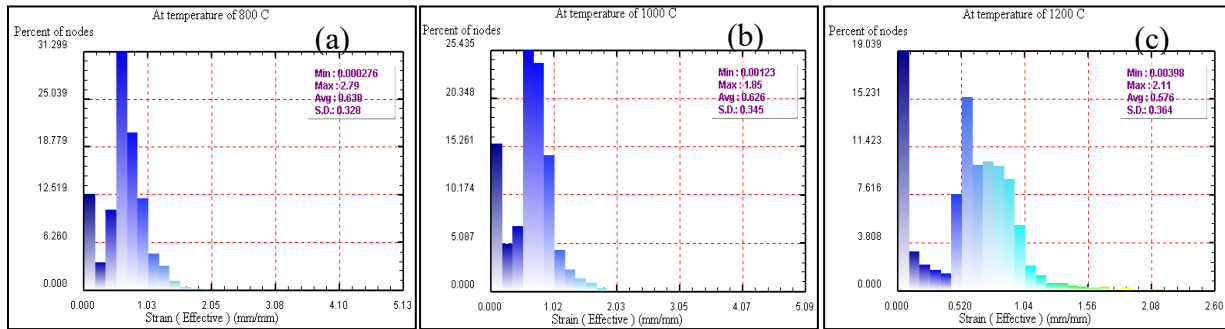


Fig. 13 Effect of die movement on the effective strain distribution

Conclusion

The hot forging of AISI 4120 alloy steel at different temperatures (800 °C, 1000 °C, and 1200 °C) was modeled using a computer simulation. 3D Deform version 11 was used to explore the impacts of effective strain, effective stress, displacement, flow velocity, and ultimate temperature. As a result of this experiment, the following observations were made:

- The effective strain and stress decreased when the forging temperature increased with 200° C intervals from 800° C to 1200° C, resulting in less plastic deformation and less refinement of grain structure.
- The total displacement and velocity decreased, leading to higher billet forging resistance.
- The smallest effective strain was observed at maximum effective stress.
- As the temperature increases, the minimum load is necessary, as is the case in the forging industry.
- Material deformation may be easily anticipated using computer simulation, providing a superior solution for the forging industry.

Acknowledgment

This research was supported by INDMET project; grant number 62862 funded by the NORHED II program. The authors would like to acknowledge this financial support.

References

- [1] B.V. Kiefer and K.N. Shah, "Three-dimensional simulation of open-die press forging," *J. Eng. Mater. Technol. Trans. ASME*, vol. 112, no. 4, pp. 477–485, 1990, doi: 10.1115/1.2903360.
- [2] Y. Zhang, J. Huang, X. Lin, and Q. Fang, "Numerical simulation analysis on cold closed-die forging of differential satellite gear in car," *Mater. Sci. Forum*, vol. 575-578 PART 1, pp. 517–524, 2008, doi: 10.4028/www.scientific.net/msf.575-578.517.
- [3] F. J. Olivares, A. M. Camacho, and M. A. Sebastián, "Analysis comparative of different simulation techniques by the finite element method in the study of an open die forging process," *AIP Conf. Proc.*, vol. 1431, no. August 2015, pp. 668–675, 2012, doi: 10.1063/1.4707622.
- [4] I. Poláková, M. Duchek, and L. Malencek, "FEM simulation of open die forging of a plate from material NIMONIC 80A in DEFORM 3D," *Arch. Mater. Sci. Eng.*, vol. 66, no. 1, pp. 31–36, 2014.
- [5] Y. Cheng, X. Yang, Q. Lu, C. V. S. Lim, and A. Huang, "Sensitivity analysis of process parameters for developing an improved open die forging process," *Key Eng. Mater.*, vol. 622–623, pp. 231–238, 2014, doi: 10.4028/www.scientific.net/KEM.622-623.231.
- [6] I. L. Konstantinov, I. Y. Gubanov, I. O. Astrashabov, S. B. Sidel'nikov, and N. A. Belan, "Simulation of die forging of an AK6 aluminum alloy forged piece," *Russ. J. Non-Ferrous Met.*, vol. 56, no. 2, pp. 177–180, 2015, doi: 10.3103/S1067821215020108.
- [7] V. . Kukhar, V.V., Nikolenko, R.S. and Burko, "Analysis of die-forging variants of geometrically complex forgings in Deform 3D package," *Metall. Min. Ind.*, vol. 1, no. 1, pp. 18–24, 2016, [Online]. Available: internal-pdf://90.53.138.100/4_Kukhar.pdf
- [8] Z. Li, B. Wang, W. Ma, and L. Yang, "Comparison of ironing finishing and compressing finishing as post-forging for net-shape manufacturing," *Int. J. Adv. Manuf. Technol.*, vol. 86, no. 9–12, pp. 3333–3343, 2016, doi: 10.1007/s00170-016-8424-8.
- [9] D. J. Politis, N. J. Politis, J. Lin, and T. A. Dean, "A review of force reduction methods in precision forging axisymmetric shapes," *Int. J. Adv. Manuf. Technol.*, vol. 97, no. 5–8, pp. 2809–2833, 2018, doi: 10.1007/s00170-018-2151-2.
- [10] P. Shi, X. Xia, J. Zhou, and P. Xiao, "Simulation Analysis of Forging Process of Automobile Aluminum Alloy Swing Arm," *IOP Conf. Ser. Mater. Sci. Eng.*, vol. 562, no. 1, 2019, doi: 10.1088/1757-899X/562/1/012139.
- [11] S. Joshy, A. Anil, V. M. Akshay, A. M. Chandy, and B. Nair, "Influence of Die Temperature on Die Stress Analysis Using Deform 3D," *Int. J. Mechatronics Manuf. Technol.*, vol. 5, no. 1, pp. 14–30, 2020.
- [12] J. O. Obiko, F. M. Mwema, and H. Shangwira, "Forging optimisation process using numerical simulation and Taguchi method," *SN Appl. Sci.*, vol. 2, no. 4, pp. 1–9, 2020, doi: 10.1007/s42452-020-2547-0.
- [13] Š. Hajdu, "Numerical simulation of forging process in deform 3d," *Mater. Sci. Forum*, vol. 994, pp. 256–264, 2020, doi: 10.4028/www.scientific.net/msf.994.256.
- [14] H. C. Ji, Y. M. Li, W. D. Li, S. H. Xiao, J. S. Zhang, and Y. H. Lu, "Study on forging process of valve based on response surface method," *Metalurgija*, vol. 59, no. 3, pp. 321–324, 2020.
- [15] V. Kukhar et al., "The selection of options for closed-die forging of complex parts using computer simulation by the criteria of material savings and minimum forging force," *Adv. Intell. Syst. Comput.*, vol. 989, pp. 325–331, 2020, doi: 10.1007/978-981-13-8618-3_35.
- [16] S. Jana, J. Mukhopadhyay, R. Rao, and V. Meka, "Open Die Forging Simulation of Superalloy NIMONIC 115 Using DEFORM 3D Software," In *TMS 2021*. Springer International Publishing, 2021. doi: 10.1007/978-3-030-65261-6_74.

-
- [17] Y. qiang Wu and K. kun Wang, "The ultra-high temperature forging process based on DEFORM-3D simulation," *Int. J. Interact. Des. Manuf.*, vol. 16, no. 1, pp. 99–108, 2022, doi: 10.1007/s12008-021-00811-y.
- [18] Z. J. Zhang, G. Z. Dai, S. N. Wu, L. X. Dong, and L. L. Liu, "Simulation of 42CrMo steel billet upsetting and its defects analyses during forming process based on the software DEFORM-3D," *Mater. Sci. Eng. A*, vol. 499, no. 1–2, pp. 49–52, 2009, doi: 10.1016/j.msea.2007.11.135.
- [19] X. Hua, G. Xiao-long, and J. Cheng-cheng, "Numerical Simulation of Blank-making Roll Forging Process for Heavy Automotive Front Axle," no. *Mems*, pp. 481–484, 2012, doi: 10.2991/mems.2012.86.
- [20] A. L. I. Moraes and O. Balancin, "Numerical simulation of hot closed die forging of a low carbon steel coupled with microstructure evolution," *Mater. Res.*, vol. 18, no. 1, pp. 92–97, 2015, doi: 10.1590/1516-1439.273114.
- [21] J. O. Obiko, F. M. Mwema, and M. O. Bodunrin, "Finite element simulation of X20CrMoV121 steel billet forging process using the Deform 3D software," *SN Appl. Sci.*, vol. 1, no. 9, pp. 1–10, 2019, doi: 10.1007/s42452-019-1087-y.
- [22] J. Obiko, F. Mwema, and E. T. Akinlabi, "Strain rate-strain/stress relationship during isothermal forging: A deform-3D FEM," *Eng. Solid Mech.*, vol. 8, no. 1, pp. 1–6, 2020, doi: 10.5267/j.esm.2019.9.003.
- [23] K. V. D. Rajesh and T. Buddi, "Finite element analysis of chromium and nickel alloyed steel billets forged under warm forming process using Deform-3D," *Adv. Mater. Process. Technol.*, vol. 8, no. sup3, pp. 1386–1394, 2022, doi: 10.1080/2374068X.2021.1945269.
- [24] K. V. D. Rajesh, T. Buddi, and H. Mishra, "Finite Element Simulation of Ti-6Al-4V Billet on open die forging process under different temperatures using DEFORM-3D," *Adv. Mater. Process. Technol.*, vol. 8, no. 2, pp. 1963–1972, 2022, doi: 10.1080/2374068X.2021.1878708.
- [25] A. Jayanthi, M. Anilkumar, and B. Ravisankar, "Study on multi stage forging process with combination of different strain rate and temperature region in IMI685 aero engine compressor disc forging," *Mater. Today Proc.*, vol. 60, pp. 1973–1980, 2022, doi: 10.1016/j.matpr.2022.01.208.
- [26] B. Deepanraj, N. Senthilkumar, G. Hariharan, T. Tamizharasan, and T. Tefera Bezabih, "Numerical Modelling, Simulation, and Analysis of the End-Milling Process Using DEFORM-3D with Experimental Validation," *Adv. Mater. Sci. Eng.*, vol. 2022, 2022, doi: 10.1155/2022/5692298.
- [27] M. R. Rahul, S. Samal, S. Venugopal, and G. Phanikumar, "Experimental and finite element simulation studies on hot deformation behaviour of AlCoCrFeNi2.1 eutectic high entropy alloy," *J. Alloys Compd.*, vol. 749, pp. 1115–1127, 2018, doi: 10.1016/j.jallcom.2018.03.262.
- [28] S. Fluhrer, "DEFORM 2D v10.2 system manual," *Notes (Manual)*, no. 614, pp. 1–288, 2011.
- [29] S. Deb, M. B. Abhilash, R. J. Immanuel, and S. K. Panigrahi, "Improved structural uniformity and specific strength of commercially pure aluminum through variable temperature multi axial forging: Finite element analysis and experimental study," *Int. J. Light. Mater. Manuf.*, vol. 6, no. 3, pp. 434–449, 2023, doi: 10.1016/j.ijlmm.2023.02.001.
- [30] R. W. Evans and P. J. Scharning, "Axisymmetric compression test and hot working properties of alloys," *Mater. Sci. Technol.*, vol. 17, no. 8, pp. 995–1004, 2001, doi: 10.1179/026708301101510843.
- [31] Y. P. Li, E. Onodera, H. Matsumoto, and A. Chiba, "Correcting the stress-strain curve in hot compression process to high strain level," *Metall. Mater. Trans. A Phys. Metall. Mater. Sci.*, vol. 40, no. 4, pp. 982–990, 2009, doi: 10.1007/s11661-009-9783-7.